Synthesis, characterization, and assessment of the antimicrobial activity of MgO – calcium alginate porous beads

Síntesis, caracterización y evaluación de la actividad antimicrobiana de las cuentas porosas de MgO - alginato de calcio

Yarilyn Cedeño-Mattei [1,2], Oscar Perales-Pérez [3*]

[1] University of Puerto Rico – Ponce Campus, Department of Chemistry and Physics, Ponce, Puerto Rico
[2] Interamerican University of Puerto Rico – San Germán Campus, Department of Biology, Chemistry, and Environmental Sciences, San Germán, Puerto Rico
[3] University of Puerto Rico – Mayagüez Campus, Department of Engineering Sciences and Materials, Mayagüez, Puerto Rico

Recibido : 15/10/2016 Aceptado: 30/11/2016

RESUMEN

La dispersión de nanopartículas antibacterianas en matrices poliméricas biocompatibles, no tóxicas y biodegradables permitirá el desarrollo de materiales más eficientes y efectivos para la conservación de alimentos, la eliminación de contaminantes y la protección contra microorganismos que comprometen la salud humana. Los materiales bactericidas nanométricos tienen una relación superficie / volumen muy grande que les permite interactuar con más copias de moléculas biológicas, y por lo tanto, mejorar la eficacia antimicrobiana. Más recientemente, se ha sugerido la actividad antimicrobiana del MgO amigable con el medio ambiente y químicamente estable. La incorporación de compuestos bactericidas en una matriz polimérica puede combinar la estabilidad física proporcionada por la matriz polimérica con las propiedades antimicrobianas de los agentes antimicrobianos dispersados como partıculas pequeñas sólidas. Sobre esta base, la presente investigación se centrará en el desarrollo de mezclas de partículas inorgánicas poliméricas biocompatibles, los denominados nanocompuestos, con actividad antimicrobiana sintonizable y mejorada. Se confirmó la actividad antimicrobiana de perlas de alginato cálcico - MgO (que oscilaban entre 0% y 40% p / p MgO) contra E. coli. Las perlas que contenían 20% p / p de MgO inhibían completamente el crecimiento bacterial de la E. coli

Palabras Clave: Alginato de calcio, Cuentas porosas, Óxido de magnesio, Actividad antimicrobiana

ABSTRACT

The dispersion of antibacterial nanoparticles into bio-compatible, non-toxic and bio-degradable polymeric matrices will enable the development of more efficient and effective materials for food preservation, removal of contaminants, and protection against human health-compromising microorganisms. Nanometric bactericidal materials have a very large surface to volume ratio that enable them to attach more copies of biological molecules, and hence, enhance antimicrobial efficiency. More recently, the antimicrobial activity of environmental-friendly and chemically stable MgO has been suggested. The incorporation of bactericidal compounds into a polymeric matrix can combine physical stability provided by the polymeric matrix with the antimicrobial properties of antimicrobial agents dispersed as solid tiny particles. On this basis, the present research will be focused on the development of biocompatible polymer-inorganic particle mixtures, so-called nanocomposites, with tunable and enhanced antimicrobial activity. The antimicrobial activity of calcium alginate – MgO beads (ranging from 0% - 40% w/w MgO) against *E. coli* was confirmed. Beads containing 20% w/w of MgO fully inhibited the *E. coli*. bacterial growth.

Keywords: Calcium alginate, Porous beads, Magnesium oxide, Antimicrobial activity

1 Introduction

Polymer nanotechnology involves the research and development in the design, manufacture, processing and application of polymeric materials hosting particles or devices that have one or more dimensions below 100 nm [1]. Novel and more efficient composites based on biodegradable polymer nanotechnology will provide innovative and safe alternatives to any critical interaction with human health while reducing the

* Corresponding author:
E-mail: oscarjuan.perales@upr.edu
DOI: http://dx.doi.org/10.21754/tecnia.v26i2.52

reduction of volume of waste material to be disposed in landfills.

Biopolymers, such as calcium alginate, represent an alternative to common, but minimally recycled, plastics. Previous studies demonstrated the attractiveness of antimicrobial formulations within biopolymers in the form of nanoparticles [2]; TiO_2, ZnO, Ag, carbon nanotubes, and MgO have been proposed as antimicrobial agents. Additionally, the processing of materials at the nanoscale enables the tuning in the bactericide capacity as function of particle size and concentration.

Magnesium oxide is a promising nanomaterial with strong antimicrobial effect which can be embedded into calcium alginate porous beads for water disinfection applications. MgO can inactivate microbial by forming superoxide ($O2\bullet^-$), a reactive oxygen species (ROS) [3]. It has been proved that MgO has almost the same antimicrobial effect on Gram-negative and Gram-positive bacteria [4]. Pathogen inactivation might depend on factors like: close contact of MgO particles with bacteria, alkaline condition of the particle surface, particle specific surface area, contact time and availability of active oxygen onto nanoparticles surface. ROS generally attacked carbonyl group of peptide linkages and eventually promoted the degradation of protein. Smaller particle size might produce more superoxide ions and accelerate the destruction of bacteria [4]. ROS generally work by destructing cell membrane, damaging DNA and protein, releasing hazardous ions for cell malfunction, disrupting electron transfer and hampering respiration process [5].

MgO can inactivate the pathogens by forming ROS; however, adsorption process or direct cell membrane penetration by the particles may be other possible ways for pathogens inactivation.

On the other hand, the safe handling of isolated nanomaterials in any system will be a challenging task, unless they are immobilized inside some macroscopic, eco-friendly and porous matrix. Accordingly, the synthesis, characterization, and assessment of the antimicrobial activity of MgO – calcium alginate porous beads will be addressed in the present publication.

2 Experimental

2.1 Materials

All regents were of analytical grade and used without any further purification. $Mg(NO_3)_2$ (ACS, 98-102%, Alfa Aesar), Na_2CO_3 (≥ 99%, Sigma-Aldrich), and NaOH (pellets, 98%, Alfa Aesar) were used for the synthesis of the magnesium carbonate hydroxide precursor. The polymeric beads were prepared using Low-Viscosity Alginic Acid Sodium Salt (MPI Biomedicals). Calcium chloride dehydrate (Fisher Scientific) was used for the crosslinking of alginate beads.

2.2 Synthesis of Magnesium Hydroxide Carbonate Precursor and MgO Nanocrystals

The synthesis of magnesium carbonate hydroxide (hydromagnesite, MCH) precursor was carried out by the modification of the route proposed by Y. Zhao *et al.* [6], involving separate nucleation and aging steps in aqueous phase. Solution-1 consisted of 100 mL 0.3 M $Mg(NO_3)_2$, while solution-2 contained 100 mL of stoichiometric amounts of Na_2CO_3 and NaOH. Solutions 1 and 2 were added simultaneously into the reaction vessel and homogenized at 11000 rpm for 2 minutes (nucleation step). The resulting slurry is stirred and heated at 100°C for different reaction times (aging step). The aged precipitate was washed three times with deionized water and dried at 50 °C for 24 hours. The formation of the hydromagnesite is explained by the following reaction:

$$5Mg(NO_3)_2 + 4Na_2CO_3 + 2NaOH \xrightarrow{\Delta} 4MgCO_3{\cdot}Mg(OH)_2{\cdot}4H_2O + 10NaNO_3 \quad (1)$$

The synthesized magnesium carbonate hydroxide precursor was thermally treated to develop the MgO phase. This is a three-step process based in the dehydration, dehydroxilation, and decarbonation of the precursor, which leads to:

$$4MgCO_3{\cdot}Mg(OH)_2{\cdot}4H_2O \xrightarrow{\Delta} 5\ MgO + 5\ H_2O + 4\ CO_2 \quad (2)$$

The thermal decomposition of hydromagnesite is expected to proceed via three stages [7]:

Dehydration (removal of water of crystallization):

$$4MgCO_3{\cdot}Mg(OH)_2{\cdot}4H_2O \rightarrow 4MgCO_3{\cdot}Mg(OH)_2 + 4H_2O \quad (< 250\ °C) \quad (3)$$

Dehydroxylation (decomposition of magnesium hydroxide to MgO):

$$4MgCO_3{\cdot}Mg(OH)_2 \rightarrow 4MgCO_3 + MgO + H_2O \quad (250 – 350\ °C) \quad (4)$$

Decarbonation (decomposition of magnesium carbonate to MgO):

$$4MgCO_3 \rightarrow 4MgO + 4CO_2 \quad (>350\ °C) \quad (5)$$

The total theoretical mass loss expected for hydromagnesite is 56.9%. This corresponds to a theoretical mass loss of 19.3% (below 350 °C) and 37.6% (above 350 °C).

2.3 Synthesis of Calcium Alginate and MgO – calcium alginate porous beads

A 2% w/w sodium alginate solution was contacted with a $CaCl_2{\cdot}2H_2O$ 0.2 M solution using a peristaltic

pump. The crosslinking leads to the development of the well-known egg box structure of the biopolymer. The formed beads are magnetically stirred in solution for 30 minutes, collected and rinsed with distilled water and dried at room temperature. In order to prepare MgO – calcium alginate nanocomposite beads, MgO is dispersed into the Na-alginate precursor using a homogenizer at 11000 rpm. The w/w MgO loading was evaluated in the 0% - 40% w/w range. The resulting solution is dripped into calcium chloride for crosslinking.

2.4 Nanocrystals Characterization

The crystalline structure of MgO nanocrystals was investigated using a Siemens D500 X-Ray Diffractometer with Cu K_α radiation. The average crystallite size was calculated using the Scherrer's equation. The size of the beads was examined using a Nikon SMZ1500 Stereozoom Microscope. A Shimadzu IRAffinity-1 Fourier Transformed Infrared Spectrophotometer was used to confirm the formation of the desired structures.

2.5 Assessment of the Antimicrobial Activity

The antimicrobial activity of MgO – calcium alginate porous beads was assessed by the Spread Plate Method [8]. The capacity for inhibition of bacterial growth was assessed in presence of 0.1 g and 0.25 g of nanocomposite. A fixed volume of 100 µL of the inoculum of *E.coli* or *Salmonella* at a concentration of 10^8 cells/mL was mixed with the different masses of nanocomposite and the final volume was filled up to 10 mL by using Tryptic Soy Broth (TSB). A negative control was examined in absence of nanoparticles. The test units were placed in an incubator at 37°C in darkness. Each treatment was run by triplicate. After 24 hours of incubation, the samples were diluted until a dilution factor of 10^8 was reached. A small amount of the bacterial suspension was spread over the Mueller Hinton agar (*E. coli*) or Xylose lysine deoxycholate (XLD) (*Salmonella*) surface and incubated at 37 °C for 24 hours to permit the growth of colonies. The colonies were subsequently quantified and multiplied for the corresponding dilution factor.

The Singlet Oxygen Sensor Green (SOSG) reagent kit was used to detect the generation of one of the ROS species (i.e. singlet oxygen).

3 Results and Discussion

3.1 X-Ray Diffraction (XRD) Analyses

Figure 1 shows the XRD patterns of the powders of magnesium carbonate hydroxide precursor aged for one hour and MgO nanocrystals formed after thermal treatment in air at 600 °C for one hour. One hour of aging was conducive to the formation of well crystallized magnesium carbonate hydroxide (hydromagnesite) precursor compound. In turn, the presence of diffraction peaks corresponding to the (111), (200), and (220) crystallographic planes of cubic MgO-periclase became evident. The lattice parameter for the sample synthesized after one hour of thermal decomposition was estimated at 4.22 Å, which is in good agreement with the bulk value for MgO (4.21 Å) [9]. The average crystallite size of MgO synthesized from the hydromagnesite was 13 ± 1 nm.

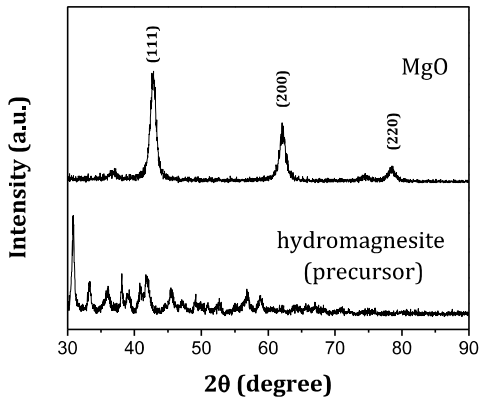

FIGURE 1. X-Ray Diffraction patterns of hydromagnesite aged for 1 hour and MgO powders thermally treated for one hour.

3.2 Characterization of calcium –alginate porous beads

Figure 2 shows the actual calcium alginate – MgO beads synthesized. Spherical beads are obtained for 5% w/w MgO content and below. An increase in MgO loading leads to the formation of flake-like structures (10 – 40%).

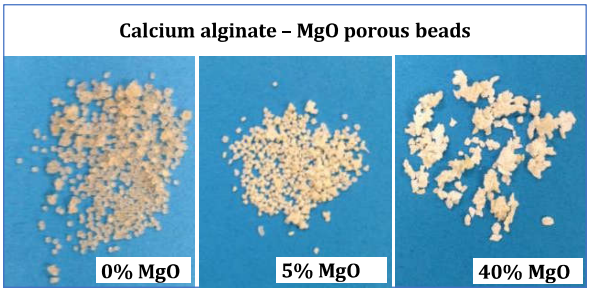

FIGURE 2. Bare calcium alginate beads (left), MgO – calcium alginate beads containing 5% (center), and 40% MgO (right).

3.3 Stereomicroscope images

Stereomicroscope images corresponding to calcium alginate beads (a) and calcium alginate – MgO porous beads (b) are shown in Figure 3. The average size of calcium alginate – 5% w/w MgO beads was 1.7 mm while the bare calcium alginate beads were more compact

(1.4 mm of average diameter) and showed less porosity than those containing MgO.

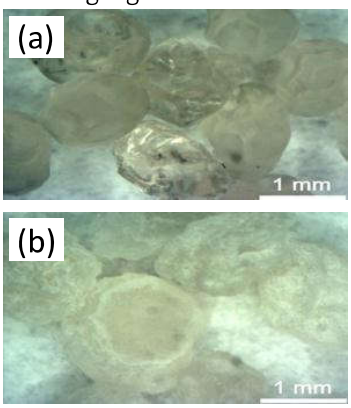

FIGURE 3. Stereomicroscope images of calcium alginate beads (a) and 5% w/wMgO – calcium alginate beads (b).

3.4 Fourier Transformed - Infrared Spectroscopy Measurements of calcium alginate – MgO beads

IR spectra (Figure 4) confirmed that the alginate structure remains unaltered after processing and fabrication of the porous beads and it is independent of the MgO content. The broad band at 3300 cm^{-1} corresponds to stretching vibrations of O–H bonds of alginate. The asymmetric and symmetric stretching vibrations of carboxylate salt ion are located at 1592 and 1411 cm^{-1} and the C–O stretching vibration is located at 1024 cm^{-1}. The band at 550 cm^{-1} corresponds to the metal–oxygen vibration. It could be attributed either to MgO or Ca–O due to the egg box conformation of the biopolymer.

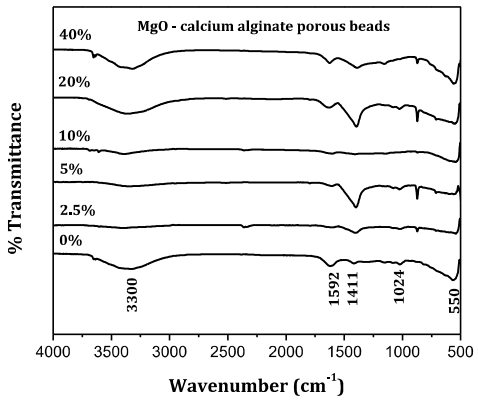

FIGURE 4. IR spectra of calcium alginate – MgO porous beads.

3.5 Antimicrobial Activity of calcium alginate – MgO porous beads against *E. coli* and *Salmonella*

Figure 5 shows MacConkey agar plates corresponding to the *E. coli* growth inhibition in absence (left) and presence of 0.1g (center) and 0.25 g (right) of 20% w/w MgO – calcium alginate porous beads. As seen, a complete bacterial growth inhibition was attained for 0.25 g of beads containing 20% w/w MgO. A full summary of the *E. coli* growth inhibition in presence of 0.1 g or 0.25 g of the nanocomposite and several MgO content is summarized in Table 1.

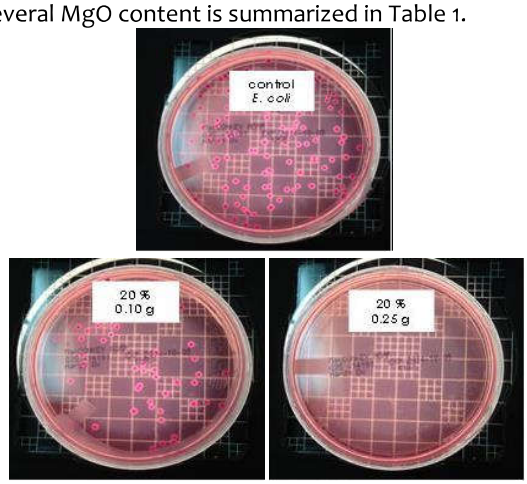

FIGURE 5. MacConkey agar plates showing *E. coli* colonies after contacting the bacteria with different weights of 20% w/w MgO-Ca alginate nanocomposite beads. The control test (i.e. no presence of the nanocomposite) is also shown for comparison purposes .

TABLE 1. Bacterial growth inhibition percentage for *E. coli* in presence of: calcium alginate – MgO beads synthesized at different MgO w/w loadings. The bacteria were contacted with 0.1 and 0.25 g of each nanocomposite sample.

MgO Content (%)	Beads (g)	Bacterial growth inhibition (%)
0	0.1	3
	0.25	20
2.5	0.1	8
	0.25	15
5	0.1	21
	0.25	33
10	0.1	14
	0.25	24
20	0.1	59
	0.25	100
40	0.1	100
	0.25	100

An increasing inhibitory tendency in bacteria growth was evidenced as the MgO loading and/or nanocomposite mass increases.

FIGURE 6. XLD agar plate showing *Salmonella* colonies (control test).

Figure 6 shows the XLD agar plates containing the characteristic red colonies with black center of *Salmonella*. The MgO – calcium alginate beads were incubated in presence of *Salmonella* and the summary of results is presented in Table 2. A (-) minus sign means that the bacterial population increased instead of being inhibited.

TABLE 2. Bacterial growth inhibition percentage for *Salmonella* in presence of: calcium alginate – MgO beads synthesized at different MgO w/w loadings. The bacteria were contacted with 0.1 and 0.25 g of each nanocomposite sample.

MgO Content (%)	Beads (g)	Bacterial growth inhibition (%)
5	0.1	-21
	0.25	8
10	0.1	5
	0.25	19
20	0.1	-13
	0.25	31
40	0.1	99
	0.25	100

Calcium alginate - 40% MgO porous beads led to a complete bacterial inhibition against *Salmonella*. The inhibition is lower when compared to *E. coli* (20% w/w MgO beads were enough to attain a complete inhibition).

3.6 Generation of Singlet Oxygen

To detect the generation of singlet oxygen (SO) the Singlet Oxygen Sensor Green (SOSG) reagent kit was used. This reagent is highly sensitive to the presence of SO but does not show any appreciable response to hydroxyl radical or superoxide species. The SOSG initially exhibited a weak blue fluorescence, with emission peaks at 395 and 416 nm (excitation at 372 and 393 nm, respectively). SOSG emits a green fluorescence in the presence of SO with excitation/emission maxima around 504/525 nm. The intensity of the green-fluorescent signal is correlated with SO concentration with insignificant interference from another ROS. The SOSG was used to determine the generation of SO by the 13 nm MgO nanoparticles. Figure 7 (a) shows the Photoluminescence (PL) spectra of the blank. As seen, there is no considerable variation in the PL intensity by prolonging the exposure time. On the contrary, the PL spectra of Figure 7 (b) evidences the significant increment in the emission peak intensity by increasing the illumination time, which is attributed to the generation of SO by the MgO nanoparticles. The SO generation increased 2.5 times when MgO nanoparticles were present.

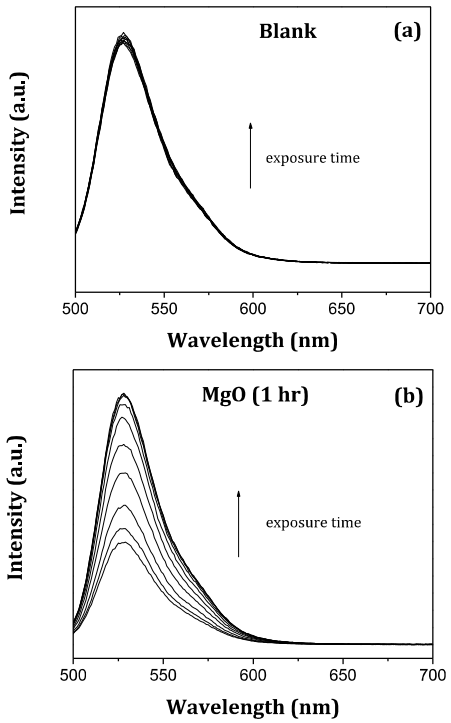

FIGURE 7. Photoluminescence (PL) spectra of the singlet oxygen sensor green (a) without MgO nanoparticles (blank), and (b) in presence of 13 nm MgO nanoparticles.

4 Conclusions

MgO – calcium alginate porous beads were successfully synthesized in the 0 - 40% w/w range. FT- IR spectroscopy confirmed that the calcium alginate structure remained unaltered after the beads

fabrication. MgO content above 10% w/w led to flake-like structures. The antimicrobial activity of calcium alginate – MgO beads against *E. coli* and *Salmonella* was also confirmed. Beads containing 20% w/w or 40% w/w of MgO fully inhibited the *E. coli* and *Salmonella*, respectively, bacterial growth in 100%. The bactericide mechanism could be related to the generation of SO species in presence of MgO nanoaprticles.

Acknowledgments

This material is based upon work supported by The National Science Foundation under Grant No. HRD 13455156 (CREST Phase-II program). The authors also thanks Mrs. Brenda Rodríguez for her invaluable contribution on the synthesis and characterization of the nanocomposites.

References

[1] Cha D S and Chinnan M S 2004 *Crit. Rev. Food Sci. Nutr.* **44**, 223–7
[2] Suyatma N E, Copinet A, Tighzert L and Coma V 2004 *J. Polym. Environ.* **12**(1), 1–6
[3] Huang L, Li D -Q, Lin Y -J, Wei M, Evans D G and Duan X 2005 *J. Inorg. Biochem.* **99**(5), 986–93
[4] Shi L -E, Xing L, Hou B, Ge H, Guo X and Tang Z 2010 in *Current Research, Technology and Education Topics in Applied Microbiology and Microbial Biotechnology* ed A Mendez-Vilas Formatex Research Center: Badajoz pp 361-68
[5] Hossain F, Perales-Perez O J, Hwang S and Román F 2014 *Sci. Total Environ.* **466-467**, 1047-59
[6] Zhao Y, Li F, Zhang R, Evans D G and Duan X 2002 *Chem. Mater.* **14**(10), 4286-91
[7] Botha A and Strydom C A 2001 *Hydrometallurgy* **62**, 175–83
[8] Madigan M T, Martinko J M, Dunlap P V and Clark D P 2008 *Brock Biology of Microorganisms* (13th edition) Benjamin Cummings: San Francisco p. 129
[9] Downs R T and Hall-Wallace M 2003 *Am. Mineral.* **88**, 247-50